Flow Structure and Scaling Laws in Lateral Wing-Tip Blowing

C. S. Lee,* D. Tavella,† N. J. Wood,† and L. Roberts‡
Stanford University, Stanford, California

When a thin jet sheet exits from the tip of a straight wing in the spanwise direction, the wing experiences a lift augmentation. In many cases, lateral blowing causes a lateral displacement of the tip vortices, without complicating the vortex structure. In such cases, simple scaling laws for blowing intensity and lift augmentation have been found to hold. However, in some instances blowing also produces secondary vortices, which sometimes are associated with a breakdown of the scaling laws. Flow surveys for several tip jet configurations giving rise to multiple-vortex structures were conducted in a low-speed wind tunnel. An analysis of the near wake structure in such cases indicated that the presence of strong secondary vortices provided the mechanism for the scaling-law breakdown.

Nomenclature

A	= aspect ratio
b	= span of the semispan model
c	= airfoil chord
C_L	= lift coefficient
C_{Lo}	= lift coefficient in absence of blowing
C_ℓ	= sectional lift coefficient
$C\mu$	= jet momentum coefficient
q_∞	= freestream dynamic pressure
u,v,w	= u,v,w velocity components
u_∞	= free-stream velocity
v_j	= jet exit velocity
x,y,z	= streamwise, spanwise, and transverse coordinates
α	= angle of attack
δ_j	= jet slot width
Γ	= vortex strength
ρ_j	= jet fluid density
ζ	= streamwise vorticity component

Introduction

UNDER the effect of tip blowing, a straight wing experiences an increment of lift all along the wing span, the magnitude of which depends on the blowing configuration. This phenomenon, which has been studied experimentally[1-7] and theoretically,[8,9] originates in an effective enlargement of the aspect ratio associated with the lateral displacement of the tip vortices by blowing. This phenomenon is best understood in the case of a wing with a symmetrically located jet slot and where the jet exits in a direction parallel to the span. In this case, under most conditions, the jet rolls up into a vortex that engulfs the wing tip vortex. As a result only one vortex is usually present, which is identified with the tip vortex, and is displaced outward as a result of blowing. Such outward displacement of the tip vortex can be related, through an algebraic scaling law, to jet momentum, wing aspect ratio, and angle of attack.[9]

In the majority of the tests involving symmetrical slot configurations, the theoretically derived scaling laws were followed closely, except at very small angle of attack and intense blowing. In cases of nonsymmetrical slot configurations, deviations from the scaling laws occurred more frequently. An investigation into these anomalies indicated that the characteristics of the near-wake vortical structure are closely connected to the validity of the lift-augmentation scaling laws. The objective of this work was to analyze the near-wake field in three different slot configurations to assess the effect of near-wake structures on lift-augmentation efficiency and scaling-laws applicability.

Theoretical analysis has indicated that this lift augmentation is primarily an inviscid phenomenon, based on a virtual extension of the wing span. This extension ends where the jet curls up due to the pressure difference between upper and lower surfaces.

Testing of the slant-down configuration was suggested by the possibility of enlarging the virtual extension of the wing span through slanted jet ejection. If the jet is ejected with a downward slant with respect to the spanwise direction, while maintaining a constant tip external geometry, two competing effects can be conceived. Because of a downward initial slope, analysis suggests that the jet will increase its penetration into the freestream, implying an increase in span loading (more effectiveness). On the other hand, this extension of the span is produced by a jet with a shape such that it confronts the freestream at a smaller local incidence, resulting in reduced pressure difference across the jet sheet, or equivalently reduced span loading in the neighborhood of the tip (less effectiveness). These observations would suggest that an optimum downward slant could be imparted to the jet, so as to maximize lift augmentation. An optimal downward ejection angle would also take into account the vertical component of jet thrust.

The study of the offset tip configuration, on the other hand, was motivated by the possibility of exploiting the unequal flowfields—between upper and lower surfaces—that would arise from turbulent entrainment into a jet emerging from a slot displaced from the centerline of the wing cross section. Although the phenomenon of lift augmentation by lateral blowing is to a large extent an inviscid one, it is recognized that entrainment into the jet, an essentially viscous effect, could have an effect on performance. In a symmetrically located slot, entrainment into the upper and lower sides of the jet would tend to induce forces of equal intensity and opposite direction on the wing's upper and lower surfaces. If the slot were located nearer the upper surface of the wing, it would be expected that entrainment into the upper side of the jet would be felt more strongly, producing suction forces that would contribute to the lift augmentation, and at the same time would influence the boundary layer such as to retard the onset of stall.

The theoretical analysis was capable of yielding simple scaling relationships between wing and blowing parameters as a result of assuming the presence of a single tip vortex, which

Presented in part as Paper 86-1810 at the AIAA 4th Applied Aerodynamics Conference, San Diego, CA, June 9-11, 1986; received March 30, 1987; revision received March 7, 1988.

*Postdoctoral Fellow, Department of Aeronautics and Astronautics. AIAA Member.

†Research Associate, Department of Aeronautics and Astronautics. AIAA Member.

‡Director, Department of Aeronautics and Astronautics. AIAA Fellow.

was displaced by blowing. Earlier experiments, together with this study, indicated that in most cases of symmetrical slot arrangements a single vortex is found; exceptions occur at intense blowing and very small angle of attack. In nonsymmetrical configurations, however, secondary vortices were observed in all cases. The secondary vortices interact with the tip vortex either enhancing or decreasing the lift augmentation with respect to a symmetrical configuration. It was found that in cases where the strength of at least one of the secondary vortices was a significant fraction of the primary vortex strength. the algebraic scaling laws could not be applied.

The objective of this work was to analyze the near-wake field in the different configurations and to gain understanding on the effect of near-wake structures on lift-augmentation efficiency and the applicability of the lift-augmentation scaling laws.

Experimental Apparatus And Techniques

The wind-tunnel model, shown in Fig. 1, was a rectangular wing of aspect ratio 3.14 with a 15 cm chord and a NACA 0018 airfoil section. Also shown are the cross sections of the three tips tested. Tip (a) had a symmetrically located slot with an angle of ejection of 0 deg. Tip (b) was also symmetrically located but with an angle of ejection of 20 deg. Tip (c) had a slot offset 11% of the maximum airfoil thickness from the chordline and angle of ejection of 0 deg. The symmetrical airfoil cross section enabled testing of positive (up) and negative (down) slant and offset configurations. In all cases, the slots were 0.16 cm wide and extended from 7–81% of the wing chord, giving a jet aspect ratio of 74. The measurements were conducted in a low-speed wind tunnel with a cross section of 45.7 cm × 45.7 cm at the test section and a free stream velocity of 40 m/s, giving a chord-based Reynolds number of 4×10^5. Since the purpose of the experiment was to inquire about the association of scaling-law breakdown with the wake vortex structure, the effect of tunnel interference and Reynold's number were expected to be small.

Spanwise lift distributions were estimated by chordwise integration of surface pressure measurements. The three velocity components and total and static pressures in the near wake were measured with a 0.318 cm-diam, five-hole probe mounted on a three-axis traversing gear. Surveys were carried out at stations 13%, 30%, and 140% of the chord aft of the wing trailing edge for angles of attack of 0 deg to 8 deg, and jet momentum coefficients of 0.06–0.18. The jet momentum coefficient was defined as

$$C_\mu = \rho_j v_j^2 \delta_j / q_\infty c \tag{1}$$

The measuring planes were perpendicular to the freestream velocity, and approximately 450 data points with a spacing of 0.635 cm were taken in each wake survey. All of the vortices studied in the experiments were at least seven vortex radii from the wind-tunnel wall, a distance sufficiently large that no significant wind tunnel interference with the flow structures was expected.

The possibility of combining the expected positive effects of placing the slot near the upper surface with downward slant would make it desirable to conduct measurements with an appropriate tip slot. Physical constraints in the manufacturing process, however, made the machining of a tip piece combining these two effects impossible. The interpretation of the measurements must be made keeping in mind that manufacturing constraints also impose distortions in the slanted and displaced slots when compared with the symmetrical slot. This is due to the tip piece being rounded, a requirement that arose from the demand to minimize the presence of regions of separation, that would add to the complexity of the flowfields. Because of physical constraints, the exit plane, in the slant and offset configurations, was not perpendicular to the slot inner walls. Likewise, the contraction length of the slots in the spanwise direction was different, with the consequence that

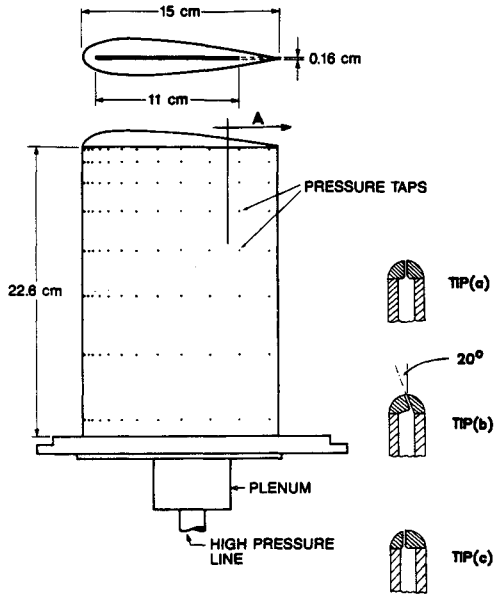

Fig. 1 Wind-tunnel model and tips.

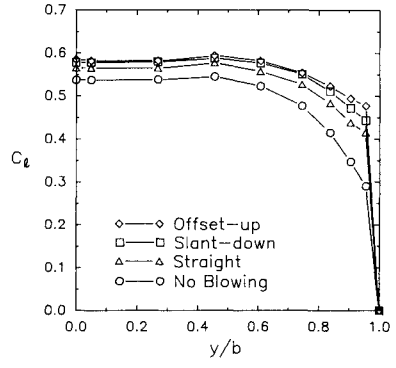

Fig. 2 Spanwise lift distribution for different configurations ($\alpha = 8$ deg, $C_\mu = 0.18$).

the velocity profiles differed slightly between the three cases.

The main sources of error are the uncertainty in angle of attack and blowing momentum coefficient, estimated to be 0.25 deg and 5%, respectively.

Discussion

Under the effect of tip blowing, the wing experiences an increment of lift all along the span, the magnitude of which depends on the tip configuration, as shown in Fig. 2. It is observed that the lift augmentations are distributed fairly uniformly along the span, consistent with a lateral displacement of the wing-tip vortices by blowing, which acts as an effective enlargement of the wing span. The enhanced suction near the tip can be attributed to viscous effects, responsible for entrainment into the jet, and is particularly noticeable in the offset case.

If only one vortex is present in the near wake, a theoretical analysis revealed that the lateral component of the vortex displacement due to blowing is given by[9]

$$\Delta b/b = k(C_\mu/C_{L_o}\, bA\alpha)^{2/3} \tag{2}$$

In this expression, k is a constant dependent on tip configuration. This displacement can be interpreted as the effective enlargement of the span as a result of blowing. In that case the lift augmentation, which is a linear function of a slight perturbation of the wing span, scales in the following way:

$$\Delta C_L/C_{L_o} = k_1 F(A)\ (C_\mu/\alpha)^{2/3} \tag{3}$$

Here k_1 is also a constant dependent on tip configuration, and $F(A)$ is a universal function of aspect ratio. The validity of this relationship also implies that the character of the lift distribution is preserved as the jet is activated and displaces the tip vortex. In particular, these scaling laws assume that the lift distribution is locally elliptical near the tip. If in the process of increasing the strength of the jet or of changing the angle of attack, secondary tip vortices appear, the lift distribution ceases to be self-preserving, since in such a case, new length scales (the distances between the primary and secondary vortices) appear. However, it may be postulated that the departure from self-preservation of lift distribution as the jet is turned on is linked to the relative strength of the secondary vortices. Weak secondary vortices would imply a relatively small departure from self-preservation, thus only slightly violating the conditions for validity of the scaling laws. Conversely, strong secondary vortices would indicate a stronger departure from the scaling laws. In addition to altering the self-similarity of the load distribution near the wing tip, secondary vortices also enhance mixing with ambient fluid, thus decreasing the ability of the tip jet to penetrate into the freestream, a further contribution to the departure from the scaling law.

The different vortex structures are illustrated in Figs. 3–6. Figure 3 shows a simple vortex structure consisting of a lateral and upward displacement of the tip vortex under blowing. Whenever this structure was present, the 2/3 power scaling law was followed closely. This structure was observed in straight blowing at angles of attack greater than 2 deg. More complex structures, containing a secondary vortex, are shown in Figs. 4 and 5. In the cases where these structures were present, deviations from the scaling law were observed and these became more marked as the relative intensity of the secondary vortex increased. These structures occurred at very small angles of attack (less than 2 deg) for straight configurations and were present, with varying degrees of strengths of secondary vortices, in all combinations of blowing intensity and angle of attack for the nonsymmetrical configurations. Figure 6 illustrates a case of multiple secondary vortices, which was observed in the unfavorable cases of slant-up and offset-down blowing configurations. In cases where these complex structures were observed, the lift-augmentation scaling law failed to apply.

The vortices present in these structures are better visualized by contour plots of the streamwise component of the vorticity, which is obtained by numerical evaluation of the crossflow velocity derivatives in the expression:

$$\zeta = \frac{\partial w}{\partial y} - \frac{\partial v}{\partial z} \tag{4}$$

where v and w were measured quantities.

Comparison of the vorticity contours, shown in Figs. 7 and 8 with the crossflow velocities in Figs. 4 and 6, indicates that

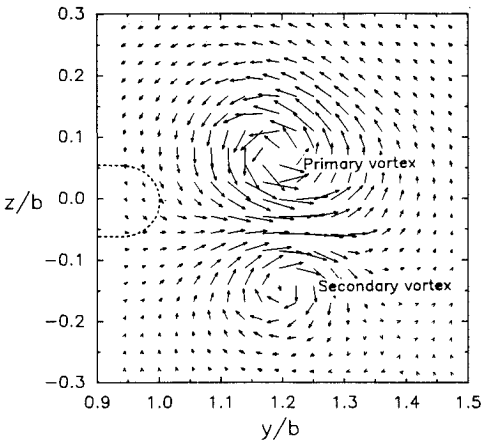

Fig. 4 Flow structure for slant-down configuration ($\alpha = 2$ deg, $C_\mu = 0.18$, $x/c = 2.4$).

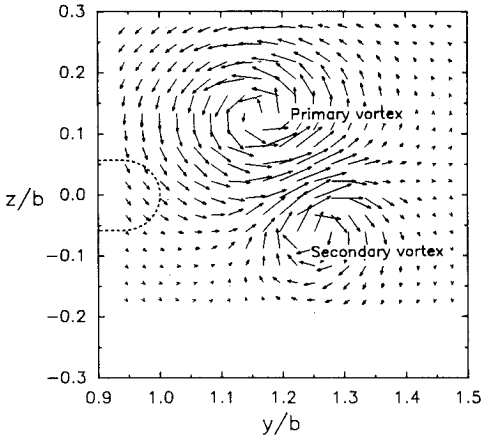

Fig. 5 Flow structure for offset-up configuration ($\alpha = 2$ deg, $C_\mu = 0.18$, $x/c = 2.4$).

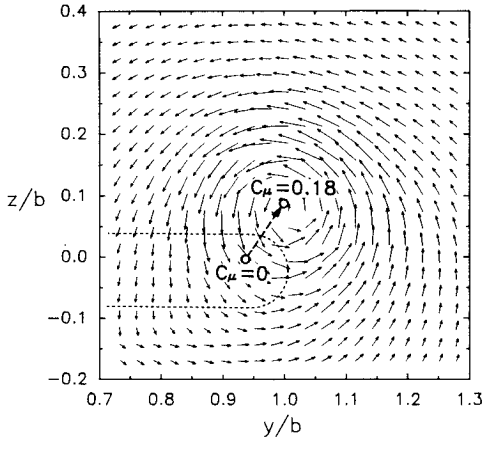

Fig. 3 Flow structure for straight configuration, intense blowing, and high angle of attack ($\alpha = 8$ deg, $C_\mu = 0.18$, $x/c = 2.4$).

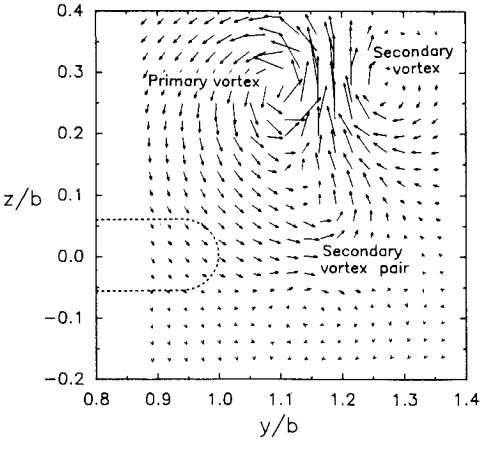

Fig. 6 Flow structure for slant-up configuration ($\alpha = 2$ deg, $C_\mu = 0.18$, $x/c = 2.4$).

the complex structure of Fig. 6 consists of four vortices. It can be seen that vorticity plots are able to reveal vortical structures difficult to distinguish from velocity plots alone.

The facts concerning deviations from the scaling law are evidenced by Figs. 9–11, corresponding to straight, slant-down, and offset-up cases. Agreement with the scaling law is generally very good for straight, slant-down, and offset-up configurations, except at angle of attack of 2 deg, with greater departures for intense blowing. It is also to be noticed that the slopes of the straight lines in these figures, numerically equal to the values of k_1 in Eq. (3), are greater for the cases of slant-down and offset-up configurations, confirming the anticipated increased performance of these two cases with respect to straight blowing. Slope evaluation gives values of k_1 of 0.108 for straight blowing, 0.134 for slant-down blowing, and 0.153 for the offset-up configuration, suggesting that differences in performance between 30–50% can be attributed to slot arrangement. The gains for the slant-down configuration is primarily an inviscid phenomenon. On the other hand, the gains for the offset-up case probably results from both viscous and inviscid effects. In this case, a greater penetration of the jet into the freestream was favored by asymmetrical entrainment into the jet. Figure 12 illustrates the drastic breakdown of the scaling law for the more complex structure of multiple secondary vortices shown in Fig. 6. No satisfactory regression can be obtained for this case.

Multiple-vortex structures are better understood by considering the individual flow components produced by a thin jet sheet into a crossflow. The relatively simple structures shown in Figs. 3–5 will be explained first. Jets of elongated cross section at a small angle to the freestream have been studied by Wu et al.[10], who observed a pair of skewed vortices with the stronger one on the leeward side. As incidence increases, the leeward vortex becomes stronger and the windward vortex becomes weaker. If the incidence of the jet sheet in a crossflow were zero, a symmetric pair of vortices would result, as in the case of a circular jet in crossflow. If the sheet is set at an angle of attack with the freestream, an additional source of vorticity for the leeward side appears in the form of a vortex representing the roll-up of the edge of the sheet. This second source of vorticity on the leeward side would be the only one present in a purely inviscid flow. In the case of the jet sheet issuing from a wing tip, yet a third source of vorticity contributes to the leeward-side vortex: the wing-tip vortex that would exist in the absence of blowing. Usually the leeward-side vortex appears as a single entity, suggesting that all three sources of vorticity for the leeward side—which are all of the same sign—coalesce into a primary vortex.

The secondary vortex, arising on the jet windward side, may or may not be present, depending on angle of attack and blowing intensity. In most instances, the secondary vortex is engulfed by the leeward vortex, this process being dependent upon the relative strengths of the primary and secondary vortices. The secondary vortex becomes visible at low angles of attack and arbitrary blowing strength, a case where the major source of vorticity of the primary vortex arises from the jet-in-crossflow effect. At higher angles of attack, the secondary vortex only becomes visible at high blowing intensities,

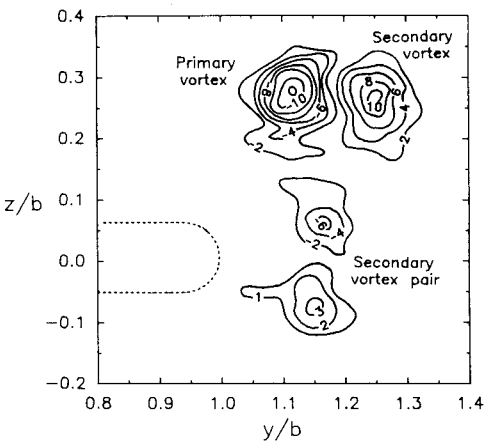

Fig. 8 Vorticity contours for slant-up configuration ($\alpha = 2$ deg, $C_\mu = 0.18$, $c/c = 2.4$).

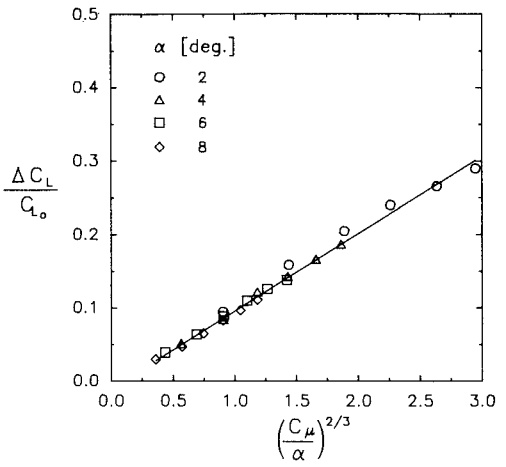

Fig. 9 Scaling law for straight blowing configuration.

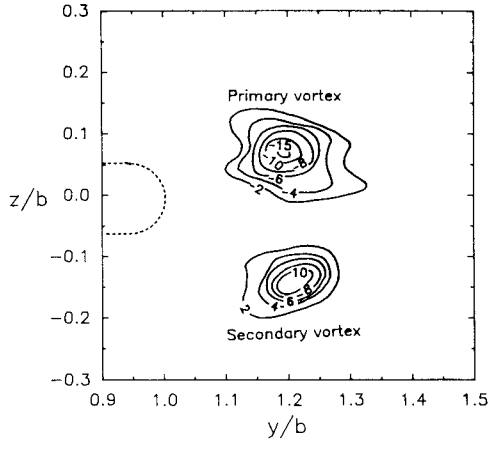

Fig. 7 Vorticity contours for straight configuration ($\alpha = 2$ deg, $C_\mu = 0.18$, $x/c = 2.4$).

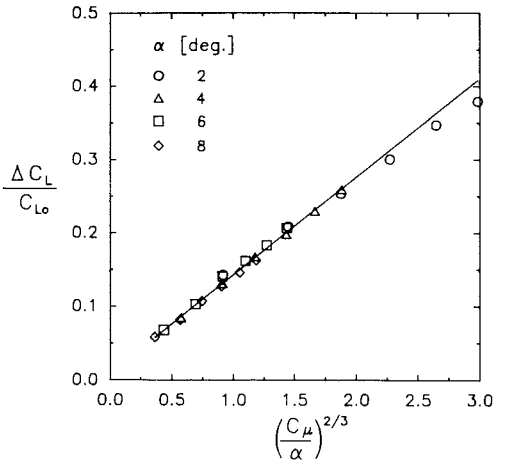

Fig. 10 Scaling law for slant-down configuration.

where the jet-in-crossflow vorticity dominates the tip vortex that would exist in the absence of blowing.

The more complex structures, found in offset-down and slant-up configurations and exemplified in Fig. 6, originated in a nonuniformity of the aft portion of the jet sheet in the proximity of the slot. This nonuniformity was due to asymmetries in the jet contraction and resulted in the jet being ripped into two separate jet sheets of different exit angle. These asymmetries resulted from manufacturing constraints, which caused the contraction length of the slot to vary along the chord. Typically, the ensuing pair of jet sheets consisted of a large front portion and a much smaller aft portion. Consequently, two pairs of counter-rotating vortices were formed, belonging to each of the two portions of the original jet sheet. The front portion displayed all of the characteristics corresponding to the jet sheet in crossflow discussed above, giving rise to the large primary vortex and the largest of the secondary vortices. The rear part produced the smaller pair, which is most clearly revealed by the vorticity contours shown in Fig. 8. The smaller pair of vortices retained its identity in the cases of slant-up and offset-down blowing due to the sense of rotation, which made a blending with the main pair unlikely. For the slant-down and offset-up configurations the smaller pair also can be presumed to have existed very near the slot, but in this case the direction of rotation of the smaller vortices favored a merging with the vortices of the main pair. In all cases of multiple vortices, the number of vortices observed was even, indicating that the inviscid tip vortex, which would exist in the absence of blowing, always blends with the leeward viscous vortex of the jet-in-crossflow effect.

It should be noted that complex structures with multiple vortices could in principle be avoided by a more precise slot design. This is not the case for the main secondary vortex, which is inherent to a jet in crossflow.

Further insight into the effects of blowing is gained by interpreting the wake in terms of vortex strengths and positions. It should be noticed that in the case of multiple vortices, the relative locations of the various vortices describe helical paths in the wake. For this reason, vortex positions were only determined for cases where relatively weak secondary vortices were identified, such that the trajectory of the primary vortex was not significantly altered.

The position of a vortex is identified as the location of maximum vorticity and the vortex strength is estimated by integrating the streamwise component of vorticity, over a cross-sectional area limited by $\zeta b/u_\infty = 1$.

Figure 13 shows that, for a symmetrical configuration, the strength of the primary vortex increases with blowing intensity and angle of attack, while the absolute value of the secondary vortex strength increases with blowing intensity and decreases with angle of attack. The same qualitative behavior was observed for the nonsymmetrical configurations, with the secondary vortex persisting over a wider range. The weakening of the secondary vortex with angle of attack is consistent with the description of elongated jets in a crossflow given above. For $\alpha > 8$ deg, the primary vortex totally engulfs the secondary vortex. The jet-in-crossflow origin of the secondary vortex is further confirmed by the approximate extrapolation indicated in Fig. 13. As the angle of attack tends to zero, both primary

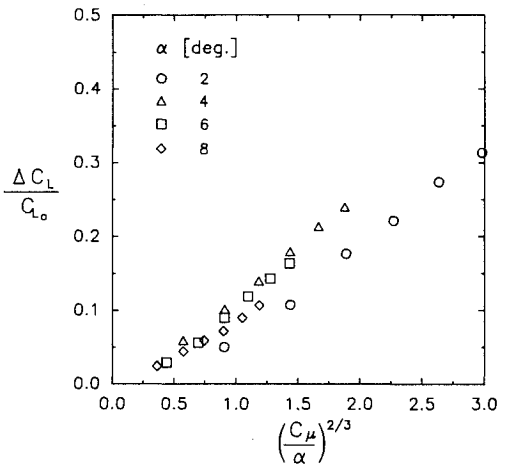

Fig. 12 Scaling law for slant-up configuration.

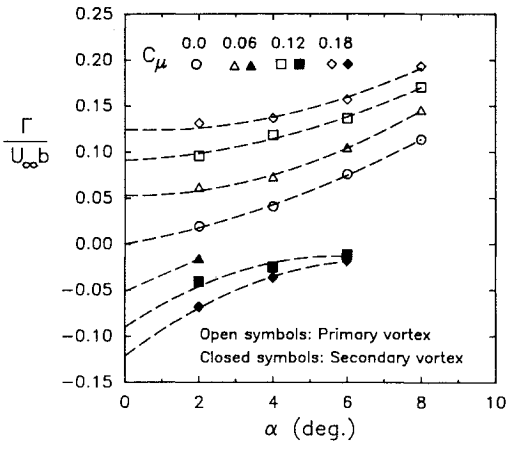

Fig. 13 Strength of the wake vortices for straight configuration ($x/c = 2.4$).

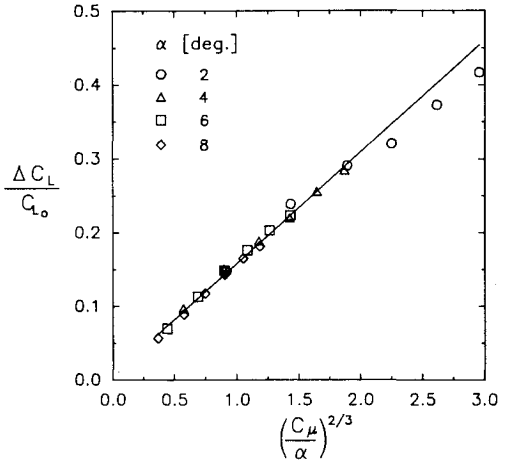

Fig. 11 Scaling law for offset-up configuration.

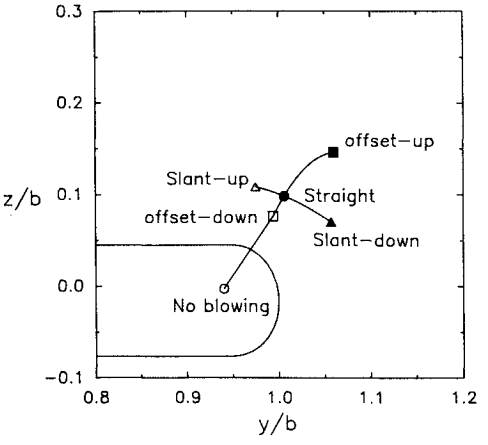

Fig. 14 Primary vortex displacement for different tip configurations ($\alpha = 8$ deg, $C_\mu = 0.18$, $x/c = 2.4$).

and secondary vortices are expected to become of equal strength and opposite sense of rotation, consistent with the jet-in-crossflow representation.

The cases of strong secondary vortex yield lower lift augmentation than predicted by the scaling law. The sense of rotation of the secondary vortex would tend to drive the primary vortex outward and to reduce the net downwash along the span, both being inviscid effects that would tend to enhance the lift augmentation. However, the presence of a secondary vortex also would tend to shorten the jet penetration into the freestream by enhancing the incorporation of freestream momentum into the jet fluid. The effect of this second mechanism dominates, causing the decrement in lift augmentation.

Figure 14 shows the displacements of the primary tip vortex for all configurations tested, at the same blowing intensity and angle of attack. Correspondingly larger lift augmentation and slope correspond to cases of larger lateral displacements of the primary vortex, in agreement with previous theoretical work.[9] This is confirmed by the lift distributions in Fig. 2 and the lift augmentations in Figs. 9–11.

Conclusions

The occasional breakdown of theoretically derived scaling laws relating lift augmentation to jet and wing parameters was found to be associated with the appearance of multiple vortices in the near wake. A severe breakdown of the scaling law was observed at very small angles of attack in association with the appearance of a strong secondary vortex. An even more serious breakdown of the scaling law was observed in association with multiple secondary vortices. The breakdowns were explained in terms of two phenomena: 1) a partial retention of some of the jet sheet momentum by the secondary vortices, decreasing the ability of the jet to penetrate into the freestream, and 2) the drastic effect of secondary vortices, particularly when more than one are present, on the self-similarity of load distribution near the wing tip assumed in the derivation of the scaling law. A consequence of secondary vortices is an alteration of the span loading as a result of modifications imparted to the downwash distribution.

References

[1]Ayers, R. F. and Wilde, M. R., "An Experimental Investigation of the Aerodynamic Characteristics of a Low Aspect Ratio Swept Wing with Blowing in a Spanwise Direction from the Tips," The College of Aeronautics, Cranfield, UK, Note 57, Sept. 1956.

[2]White, H. E., "Wind-Tunnel Investigation of the Use of Wind-Tip Blowing to Reduce Drag for Take-Off and Landing," The David Taylor Model Basin Aerodynamics Lab., AERO Rept. 1040, Jan. 1963.

[3]Briggs, M. M. and Schwind, R. G., "Augmentation of Fighter Aircraft Lift and STOL Capability by Blowing Outboard from the Wing Tips," AIAA Paper 83-0078, Jan. 1983.

[4]Wu, J. M., Vakili, A. D., and Gilliam, F. T., "Aerodynamic Interaction of Wing Tip Flow with Discrete Wing Tip Jets," AIAA Paper 84-2206, Aug. 1984.

[5]Tavella, D. A., Wood, N. J., and Harrits, P., "Influence of the Tip Blowing on Rectangular Wings," AIAA Paper 85-5001, Oct. 1985.

[6]Tavella, D. A., Lee, C. S., and Wood, N. J., "Influence of Wing Tip Configuration on Lateral Blowing Efficiency," AIAA Paper 86-0475, Jan. 1986.

[7]Lee, C. S., Tavella, D. A., Wood, N. J., and Roberts, L., "Flow structure of Lateral Wing Tip Blowing," AIAA Paper 86-1810, June 1986.

[8]Carafoli, E. and Camarasescu, N., "New Research on Small Span-Chord Ratio Wings with Lateral Jets," *Sutdii si Cercetari de Mecanica Aplicata*, Vol 29, No. 4, pp. 947–962, 1970, available in English as Translation FTD-HC-23-319, Foreign Technology Division, Air Force Systems Command, Oct. 1971.

[9]Tavella, D. A. and Roberts, L., "The Concept of Lateral Blowing," AIAA Paper 85-5001, Oct. 1985.

[10]Wu, J. M., Vakili, A. D., and Yu, F. M., "Investigation of the Interacting Flow of Nonsymmetric Jets in Crossflow," AIAA Paper 86-0280, Jan. 1986.